

Quantum interference effect and electric field domain formation in quantum well infrared photodetectors

Yuanjian Xu,^{a)} Ali Shakouri, and Amnon Yariv

Department of Applied Physics 128-95, California Institute of Technology, Pasadena, California 91125

(Received 3 February 1995; accepted for publication 17 April 1995)

An observation of quantum interference effect in photocurrent spectra of a weakly coupled bound-to-continuum multiple quantum well photodetector is reported. This effect persists even at high biases where the Kronig–Penney minibands of periodic superlattice potential in the continuum are destroyed. Our results show that electrons remain coherent over a distance of 40–50 nm. The observation was used to investigate electric field domain formation induced by sequential resonant tunneling in the superlattice. A large off-resonant energy level alignment between two neighboring wells in the high field domain was observed. © 1995 American Institute of Physics.

Recently, there has been great interest in studying optical and transport properties of multiple quantum well (MQW) structures. In these “artificial molecules,” energy quantization and wave nature of carriers have been used to design new devices and to demonstrate some basic laws of quantum mechanics, e.g., to observe minibands in the continuum of periodic potential superlattice,¹ to observe suppression of optical absorption in coupled potential wells,² and to make quantum well infrared photodetectors (QWIPs) by using minibands in the continuum.³ In this letter, we report on a new observation of a quantum interference effect in the photocurrent spectra in bound-to-continuum QWIPs. Using this effect, we analyze the electric field domain formation in the superlattice.

In a weakly coupled MQW structure with two bound states in each well (i.e., a bound-to-bound QWIP),³ the absorption spectrum is a Lorentzian shape peak corresponding to a transition between the ground state and the first excited state. The contribution of other states in the continuum above the barrier is negligible because of the oscillator strength sum rule (one-to-two transition, both states being localized in the well, has a much more significant transition dipole matrix element).

When the quantum well parameters allow only one state in the well (i.e., a bound-to-continuum QWIP), the absorption spectrum is not Lorentzian any more, the states above the barriers have a strong contribution to the absorption. Because these continuum states are extended over the barriers and several neighboring wells (depending on the coherence length of electrons), electron interference effects can be observed in the absorption spectrum. At zero bias, due to the potential translation symmetry there are well-known minibands in the continuum states of the superlattice¹ which can be calculated using, for example, the Kronig–Penney model. The miniband energy gaps, depending on the overlap of the states between neighboring wells, can be designed large enough to be observable in the absorption spectrum. However, under an applied bias, such that the voltage drop per period is bigger than these energy gaps, the miniband structure is destroyed. We will show that in a QWIP even at large

biases, one can still see some features in the photocurrent spectrum which are due to electron interference effects over one or two periods of the superlattice (40–50 nm).

The sample investigated for this study was grown by molecular beam epitaxy on a (100) semi-insulating GaAs substrate (sample 1510). It consists of 50 periods of 4 nm GaAs wells, uniformly doped with Si to $n=2\times 10^{18}$ cm⁻³, separated by 20 nm Al_{0.22}Ga_{0.78}As barriers. Due to the well-known intersubband transition selection rule, the absorption measurement was done in 45° multipass geometry.³ The experimental absorption spectrum at 79 K (limited by the experimental setup) is shown in the inset of Fig. 1. The theoretical fit was calculated by solving Schrodinger's and Poisson's equations in the envelope function approximation. The effect of exchange correlation was included through the one-particle exchange-correlation potential.⁴ Nonparabolicity was taken into account as in Ref. 5. To treat the energy eigenstates above the barrier, the MQW structure was embedded between infinitely large barriers carriers at sufficiently large distances such that the far distance boundary conditions do not affect the calculated absorption spectra.⁶

To measure the photocurrent spectrum, circular devices with 200 μ m diameter were defined by wet chemical etching. AuGe/Ni/Au was deposited onto the top and bottom n^+ -GaAs contact layers. Liftoff and alloying techniques

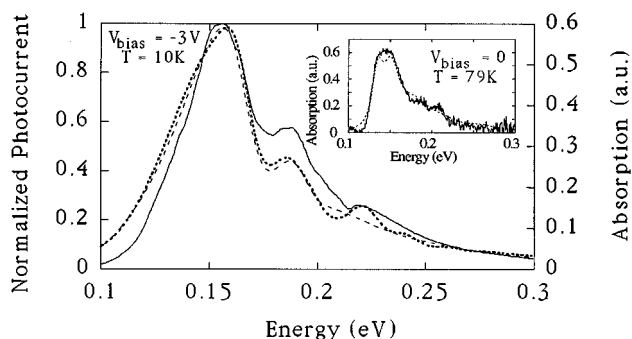


FIG. 1. The experimental photocurrent spectrum at $V_{\text{bias}} = -3$ V (solid line) and theoretical absorption spectrum (dashed line for one period and dotted line for two periods) of sample 1510 at $T = 10$ K. The inset is the experimental absorption spectrum at zero bias at $T = 79$ K (solid line) and the calculated absorption spectrum (dotted line).

^{a)}Electronic mail: yjxu@cco.caltech.edu

| Report Documentation Page | | | | Form Approved OMB No. 0704-0188 | |
|--|------------------------------------|-------------------------------------|----------------------------|---|---------------------------------|
| Public reporting burden for the collection of information is estimated to average 1 hour per response, including the time for reviewing instructions, searching existing data sources, gathering and maintaining the data needed, and completing and reviewing the collection of information. Send comments regarding this burden estimate or any other aspect of this collection of information, including suggestions for reducing this burden, to Washington Headquarters Services, Directorate for Information Operations and Reports, 1215 Jefferson Davis Highway, Suite 1204, Arlington VA 22202-4302. Respondents should be aware that notwithstanding any other provision of law, no person shall be subject to a penalty for failing to comply with a collection of information if it does not display a currently valid OMB control number. | | | | | |
| 1. REPORT DATE JUN 1995 | | 2. REPORT TYPE | | 3. DATES COVERED 00-06-1995 to 00-06-1995 | |
| 4. TITLE AND SUBTITLE Quantum interference effect and electric field domain formation in quantum well infrared photodetectors | | | | 5a. CONTRACT NUMBER | |
| | | | | 5b. GRANT NUMBER | |
| | | | | 5c. PROGRAM ELEMENT NUMBER | |
| 6. AUTHOR(S) | | | | 5d. PROJECT NUMBER | |
| | | | | 5e. TASK NUMBER | |
| | | | | 5f. WORK UNIT NUMBER | |
| 7. PERFORMING ORGANIZATION NAME(S) AND ADDRESS(ES) California Institute of Technology, Department of Applied Physics, Pasadena, CA, 91125 | | | | 8. PERFORMING ORGANIZATION REPORT NUMBER | |
| 9. SPONSORING/MONITORING AGENCY NAME(S) AND ADDRESS(ES) | | | | 10. SPONSOR/MONITOR'S ACRONYM(S) | |
| | | | | 11. SPONSOR/MONITOR'S REPORT NUMBER(S) | |
| 12. DISTRIBUTION/AVAILABILITY STATEMENT Approved for public release; distribution unlimited | | | | | |
| 13. SUPPLEMENTARY NOTES | | | | | |
| 14. ABSTRACT | | | | | |
| 15. SUBJECT TERMS | | | | | |
| 16. SECURITY CLASSIFICATION OF: | | | 17. LIMITATION OF ABSTRACT | 18. NUMBER OF PAGES 3 | 19a. NAME OF RESPONSIBLE PERSON |
| a. REPORT unclassified | b. ABSTRACT unclassified | c. THIS PAGE unclassified | | | |

were used to make Ohmic contacts. 45° mirrors were polished on the edges of the sample to couple incident infrared radiation. Figure 1 shows the photocurrent spectrum at 10 K for an applied bias of -3 V (defined with respect to the bottom contact layer). One can see three peaks at ~ 155 , 187 , and 220 meV in the photocurrent spectrum. The spacings of the peaks in the calculated absorption spectrum strongly depend on the applied field once the quantum well parameters are given. The theoretical results show only two peaks in the absorption spectrum for one quantum well, while for a quantum well with its nearest neighbors in the superlattice, there are three peaks, as shown in Fig. 1. For both of these curves, the assumed electric field on the structure is ~ 31 kV/cm. This clearly shows that the observed peaks in the photocurrent spectrum originate from electron interference effects over about two superlattice periods (a distance of 40 – 50 nm).

Although the superlattice minibands (in the Kronig–Penney sense) are destroyed at these applied biases, the physical origin of these observed peaks is that the dipole matrix element which is basically an overlap integral between the *localized* ground state in the well and the excited states above the barrier has peaks (resonances) reflecting interferences over neighboring wells. Alternatively, this can be viewed as the *local* density of the states (i.e., density of states normalized by the amplitude of the wave function in the well region) having peaks whereas the total density of states, which shows the energy level spacings for the whole superlattice, might not have any noticeable structure.

One notices that even though the *position* and the *spacing* of the peaks in the theoretical absorption spectrum match the experimental photocurrent spectrum, it is not possible to exactly fit them together (especially in the low energy region). This is because the photocurrent spectrum involves additional effects due to electron emission from the quantum well, transport in the superlattice, and capture in a distant quantum well or in the contact layers.⁷ Energy dependence of these additional processes will affect the photocurrent spectrum.

To further substantiate the fact that these observed peaks in the photocurrent spectrum originate from the local density of states in the well region and reflect electron coherence over a few periods of the superlattice, a second device (1511) was fabricated and tested. This device has the same well width and barrier height as sample 1510, however, the barrier width was increased to 40 nm. This gives a zero bias Kronig–Penney miniband structure which is very different from that of sample 1510, but as it can be seen in Fig. 2(a), the experimental photocurrent spectrum has peaks consistent with the calculated absorption spectrum of one quantum well in the superlattice. Again this shows that the electrons are coherent over at least one period of the superlattice (~ 40 nm).

Since the electron wave constructive and destructive interferences over periods of the superlattice strongly depend on the applied field, from the position and the spacing of the photocurrent peaks one can deduce the actual applied electric field over the quantum wells. Figure 2(a) shows the theoretical absorption spectrum for an applied electric field of 12

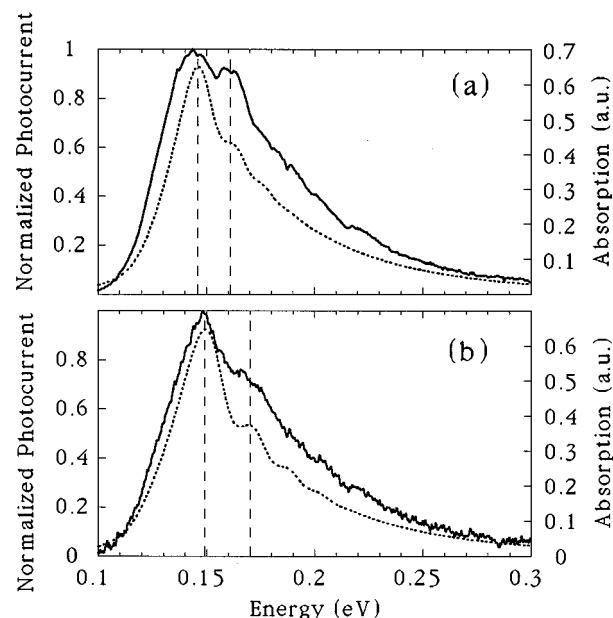


FIG. 2. The experimental photocurrent spectrum (solid line) and theoretical absorption spectrum (dotted line) at different biases of sample 1511 at $T = 10$ K. (a) $V_{\text{bias}} = -2.7$ V; (b) $V_{\text{bias}} = -3.8$ V.

kV/cm which is consistent with the experimental value of -2.7 V potential drop over 50 periods of the superlattice. When the bias is decreased to -3.8 V [Fig. 2(b)], the photocurrent peaks move (their separation increases by ~ 6 meV), the theoretical absorption spectrum which reproduces this result requires an electric field of 17 kV/cm. This is again consistent with a -3.8 V drop over 50 periods of superlattice.

The photocurrent spectrum of the sample 1510 (20 nm barriers) shows a different behavior as a function of applied bias. It shows the same three peak positions as shown in Fig. 1 for all biases between -0.2 and -4.3 V. This result is explained through the formation of electric field domains in the MQW region. In this device, because of thinner barriers, the couplings between quantum wells are stronger. It has been observed before that the conservation of lateral momentum in the tunneling process between wells induces current peaks whenever energy levels of adjacent wells are aligned.^{8–11} This leads to an instability which causes formation of high and low field domains (HFD, LFD) in the device. In the HFD, there is ground level-to-excited level sequential resonant tunneling (SRT). While in the LFD, there is ground level-to-ground level tunneling. Under illumination, the light is absorbed in all the quantum wells but only photoexcited carriers which are in a region with a high electric field have high probability of being swept out of the quantum well and contribute to the photocurrent. While those in low field region have a high probability of being recaptured by their own well, contributing negligibly to the photocurrent.

It should be noticed that the electric field (~ 31 kV/cm) for which the theoretical results match the experimental ones does not correspond to an alignment between the ground state of one well with its neighboring well's resonant state. It is a little less than half of the aligned value. Recently, Kwok

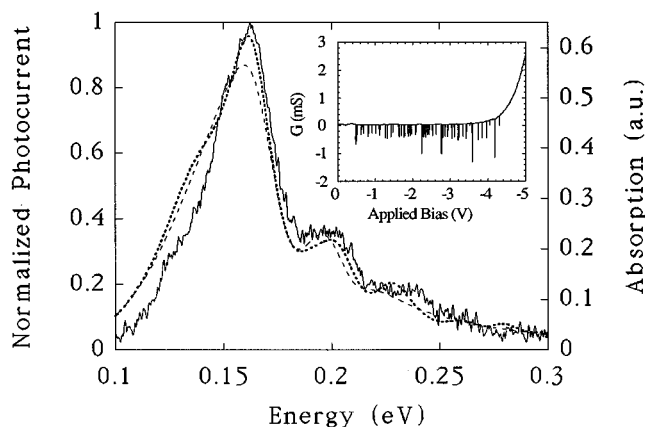


FIG. 3. The experimental photocurrent spectrum of sample 1510 at $V_{\text{bias}} = -5$ V (solid line) and theoretical absorption spectrum (dashed line for one period and dotted line for two periods) of sample 1510 at $T=10$ K. The inset is the differential conductance vs applied voltage at $T=10$ K in dark. The number of NDOs for different devices processed out of the same wafer is between 45 and 49. A second sample with exactly the same quantum well parameters as sample 1510 but with half of the number of periods shows 23–24 NDOs.

*et al.*¹¹ explained the deviation of electric field in the HFD from the resonant alignment through a current continuity model, the ~ 31 kV/cm field for the HFD in sample 1510 seems to imply that the ground state of one well is aligned with the first resonance state of the *second* nearest neighbor. At the highest bias that we could apply on the device (-5 V), the experimental result, shown in Fig. 3, shows peaks at ~ 128 , 160, 200, and 230 meV. This could be explained either by a uniform voltage drop over the structure (see the dotted curve in Fig. 3), or through the formation of a new HFD in the structure, corresponding to the alignment with higher resonance state in the second nearest-neighbor well. In the latter case, the broader peak at ~ 128 meV shows the LFD contribution. Although we cannot conclusively determine that the ground state of one well is aligned with the first resonance state of the second nearest neighbor in the HFD from this experiment, all the results are consistent with the fact that electrons remain coherent over two periods of the superlattice (for sample 1510).

Another signature of HFD formation in the sample is the oscillatory behavior in the $I-V$ characteristics which reflects more quantum wells entering the HFD region as the bias is increased.⁸ As expected, sample 1511 did not show any oscillations in the $I-V$ characteristics, but there were 48 negative differential oscillations (NDOs) for sample 1510 (see the inset in Fig. 3). This number is close to the number of quantum wells in the structure (i.e., 50). The very irregular period of these oscillations (75 ± 40 mV), might originate from the fact that for this bound-to-continuum detector, the excited levels are a series of closely spaced states above the barrier but the mean value of these oscillations is close to half of the separation between the ground state and the first resonance state.

In conclusion, we have presented a new observation of the quantum interference effect in the photocurrent spectrum which causes peaks in the latter. We estimated the coherence length of the excited electrons and analyzed the SRT induced electric field domain formation by comparing the theoretical calculation with the experimental results. A large energy level misalignment between two neighboring wells in the HFD was observed.

This work was supported by Advanced Research Projects Agency (ARPA), and by Air Force Office of Scientific Research.

- ¹D. Gershoni, J. Oiknine-Schlesinger, E. Ehrenfreund, and D. Ritter, Phys. Rev. Lett. **71**, 2975 (1993).
- ²J. Faist, F. Capasso, A. L. Hutchinson, L. Pfeiffer, and K. W. West, Phys. Rev. Lett. **71**, 3573 (1993).
- ³B. F. Levine, J. Appl. Phys. **74**, R1 (1993), and references therein.
- ⁴W. L. Bloss, J. Appl. Phys. **66**, 3639 (1989).
- ⁵D. F. Nelson, R. C. Miller, and D. A. Kleinmann, Phys. Rev. B **35**, 7770 (1987).
- ⁶Z. Ikonc, V. Milanovic, and D. Tjapkin, Appl. Phys. Lett. **54**, 247 (1989).
- ⁷F. Luc, E. Rosencher, and Ph. Bois, Appl. Phys. Lett. **62**, 2542 (1993).
- ⁸R. F. Kazarinov and R. A. Suris, Fiz. Tekh. Poluprovodn. **6**, 148 (1972) [Sov. Phys. Semicond. **6**, 120 (1972)]; L. Esaki and L. L. Chang, Phys. Rev. Lett. **33**, 495 (1974); F. Capasso, K. Mohammed, and A. Y. Cho, Appl. Phys. Lett. **48**, 478 (1986).
- ⁹K. K. Choi, B. F. Levine, R. J. Malik, J. Walker, and C. G. Bethea, Phys. Rev. B **35**, 4172 (1987).
- ¹⁰A. Shakouri, I. Grave, Y. Xu, A. Ghaffari, and A. Yariv, Appl. Phys. Lett. **63**, 1101 (1993).
- ¹¹S. H. Kwok, R. Merlin, H. T. Grahn, and K. Ploog, Phys. Rev. B **50**, 2007 (1994).